XPS and STM study of TiO2(110)-(1 x 1) surfaces immersed in simulated body fluid

Sasahara, Akira
Murakami, Tatsuya
Tomitori, Masahiko

(Citation)
Surface Science,668:61-67

(Issue Date)
2018-02

(Resource Type)
journal article

(Version)
Accepted Manuscript

(URL)
https://hdl.handle.net/20.500.14094/90004619

XPS and STM Study of TiO_2(110)-(1×1) Surfaces Immersed in Simulated Body Fluid

Akira Sasahara, Tatsuya Murakami, and Masahiko Tomitori*

Japan Advanced Institute of Science and Technology, Nomi, Ishikawa 923-1292, Japan

*To whom correspondence should be addressed.

E-mail: sasahara@harbor.kobe-u.ac.jp

Present address: Department of Chemistry, Faculty of Science

Kobe University

Nada-ku, Kobe 657-8501, Japan

Tel: +81-78-803-5674

Fax: +81-78-803-5674

Abstract

Rutile titanium dioxide (TiO_2) (110)-(1×1) surfaces prepared in ultrahigh vacuum (UHV) were removed from the UHV, immersed in Hank's buffered salt solution (HBSS), and then re-introduced to the UHV to be examined for an atomic-level study of the osteoconductivity of TiO_2. X-ray photoelectron spectroscopy (XPS) showed the adsorption of phosphate ions and divalent Ca ions from the HBSS. The density of the phosphate ions increased with the immersion time for up to 1 min and remained constant with further immersion time up to 1 week. Unlike in the case of the phosphate ions, the density of the Ca ions decreased with the immersion time after reaching the maximum value at 1 min immersion. Consequently, calcium phosphate was not formed on the (1×1) surface in the 1-week immersion. Scanning tunneling microscopy revealed molecule-sized spots covering the surfaces immersed for 1 min and longer. On the basis of density analysis by XPS, the spots were hypothesized to represent phosphate ions. Phosphate ions on the (1×1) surface are unable to undergo arrangement needed to facilitate the epitaxial growth of the brushite.

Keywords: TiO_2; calcium phosphate; STM

Introduction

Osteoconductivity is the ability for the materials to bond to bones. Implants bond to bones via the hydroxyapatite layer. This process is characteristic of Ti and its alloys, which are unique materials for replacement implants [1]. Ti-based materials are naturally coated with an oxide layer. Hence, titanium oxide is responsible for the osteoconductivity of the Ti-based materials. Hydroxyapatite is generally known to form via the calcium phosphate precursor phase, but the type and formation mechanism of the calcium phosphate have not been fully explained [2]. Clarifying the process of calcium phosphate formation would thus aid in identifying the origin of the osteoconductivity and hence allow the enhancement of the rate and/or strength of the implant–bone bonding.

Ad-species from a body fluid have been investigated by immersing titanium dioxide (TiO_2) in simulated body fluids, which are simulated balanced electrolyte solutions with ion concentrations similar to those of human plasma. Hanawa et al. examined calcium phosphate layers formed on TiO_2 films covering Ti plates [3,4]. X-ray photoelectron spectroscopy (XPS) analysis revealed a higher concentration of hydrogen phosphate ions (HPO_4^{2-}) in the calcium phosphate layer at its initial stage of growth. The authors proposed that the adsorption of the hydrogen phosphate ions and subsequent uptake of the Ca ions by the adsorbed hydrogen phosphate ions initiate the formation of calcium phosphate. The high ratio of hydrogen phosphate ions in the calcium phosphate layer agrees with the results of secondary-ion mass spectroscopy reported by Chusuei et al [5]. In this study, the authors examined the ratios of the PO_3^- and PO_2^- ions that reflect the composition of the calcium phosphate and concluded that dicalcium phosphate dihydrate ($CaHPO_4 \cdot 2H_2O$), known as brushite, is a predominant form of calcium phosphate on the TiO_2 films. On the basis of results of depth analysis by Auger electron spectroscopy, the authors propose Ca-mediated bridging between O atoms of the surface and of hydrogen phosphate ions. Kokubo et al. reported that acid treatment followed by air-annealing results in a positively charge of the Ti plates and the promoted formation of hydroxyapatite thereon [6]. According to their model, the positively charged TiO_2 surface attracts phosphate ions (PO_4^{3-}), which then lead to a negative charge of the TiO_2 surface and to the attraction of Ca and thus formation of amorphous calcium phosphate.

An atomically well-defined TiO_2 surface is expected to highlight the effect of microscopic surface structures on calcium phosphate formation. The (110) surface of rutile TiO_2 exhibits such a well-defined structure after sputter-anneal cleaning in ultrahigh vacuum (UHV) [7]. Figure 1 shows the model of the clean (110) surface with a (1×1) structure corresponding to a simple truncation of the

bulk crystal [8]. Oxygen atoms that bridge two Ti atoms, known as bridging O atoms (O_b atoms), form protruding rows along the [001] direction. Some of the O_b atoms are part of OH groups (OH_b groups), and some are missing (O vacancies) [9]. The OH_b groups are formed by the dissociation of residual H_2O molecules in the UHV chamber. At the troughs between the O_b atom rows, Ti atoms coordinated to five O atoms (Ti_{5c} atoms) are exposed. Oxygen atoms surrounding the Ti_{5c} atoms are called in-plane O atoms. The OH_t group is another type of OH group terminating the Ti_{5c} atom. It forms via the reaction of the OH_b group with O adatom (O_a atom) [10] and is absent on the (1×1) surface prepared in the UHV.

Figure 1b and 1c show empty-state images of the (1×1) surface obtained by UHV-scanning tunneling microscopy (STM). The surface consists of flat terraces separated by monatomic steps 0.33 nm high. The bright lines along the [001] direction correspond to the Ti_{5c} atom rows, and the short lines bridging the adjacent Ti_{5c} atom rows along the $[1\bar{1}0]$ direction are either OH_b groups or O vacancies. It is impossible to classify the short lines in Figure 1c into either OH_b groups or O vacancies. The image height difference between them is ~0.03 nm even in optimized imaging conditions [9]. In separate experiments, we determined the densities of the OH_b groups and the O vacancies prepared by the method in this study to be ~0.3 nm^{-2} and ~0.03 nm^{-2}, respectively [11,12]. Hence, most of the short lines in Figure 1c represent OH_b groups. The (1×1) structure has been recently found to be retained in humid environments such as laboratory air and water [13].

In this work, we examined ad-species from the Hank's buffered salt solution (HBSS), a commonly used simulated body fluid, on the TiO_2(110)-(1×1) surface. We found that the phosphate ions and the Ca ions adsorbed on the (1×1) surface and that calcium phosphate did not form after 1-week immersion. The non-formation of the calcium phosphate disagrees with the commonly known osteoconductivity of TiO_2 and suggests that the osteoconductivity is sensitive to the atomic-scale structure of the TiO_2 surface.

Experimental methods

Surface cleaning and microscope experiments were conducted using a commercial UHV-STM system (JSPM4500S, JEOL). The system is composed of the microscope chamber and the sample preparation chamber. The microscope chamber includes an STM stage, and the sample preparation chamber is equipped with an Ar^+ sputtering gun (EX03, Thermo) and low-energy electron diffraction (LEED) optics (BDL600, OCI). The base pressure of the chambers was 2×10^{-8} Pa. The view ports of the chambers were shaded unless it was necessary to view the inside.

Mirror-polished TiO_2 wafers (7 mm × 1 mm × 0.3 mm, Shinkosha) were clamped on a Si wafer that was used as a resistive heater. The surface was cleaned by cycles of sputtering with Ar ions and annealing. The ion beam energy, sample current, angle of the incident beam with respect to the surface normal, and time of the sputtering, respectively, were 2 keV, 0.5 μA, 45°, and 1 min. The temperature and time for the annealing were 1173 K and 1 min, respectively. The temperature was monitored at the side faces of the wafers by an infrared thermometer. Hence, the temperature of the TiO_2 surface was probably lower than the monitored temperature because of incomplete contact between the TiO_2 and Si wafers. The wafers with the (1×1) surface were yellowish white, similar to the as-purchased wafers, but they were also very slightly bluish, indicating that the wafers were almost stoichiometric.

The cleaned TiO_2 wafers were cooled to room temperature, removed from the sample preparation chamber, and immersed in 100 mL of HBSS (with Ca and Mg and without phenol red; Nacalai Tesque). The perfluoroalkoxy alkane container for the HBSS was shaded and was placed at room temperature. The pH of the HBSS was ~7.0 and increased to ~7.6 after 1 day of preservation in the container, regardless of the presence or absence of the TiO_2 wafer. For the 1 week immersion, the HBSS was exchanged every day. After immersion, the TiO_2 wafers were rinsed with Milli-Q water for 1 min and re-introduced to the STM system. Empty-state STM images were acquired in constant-current mode at room temperature. Electrochemically etched W wires were used as a probe.

XPS analysis was performed at room temperature using a commercial instrument (Axis Ultra DLD, Kratos). The base pressure of the system was 6×10^{-7} Pa. The TiO_2 wafers were removed from the STM system, placed in a shaded container, and transferred in laboratory air to the XPS system. A monochromatic Al Kα line was used as an excitation source. Charging of the TiO_2 surfaces was reduced by a low-energy electron neutralizer. The photoelectron emission angle θ with respect to the perpendicular line on the surface was set to 0°. The pass energy of the analyzer and the energy step were 160 and 1.0 eV for wide scans, respectively, and 20 and 0.1 eV for narrow scans, respectively. The binding energy of the spectra was calibrated such that the Ti 2p3/2 peak from Ti atoms in a bulk TiO_2 crystal was 459.1 eV. With this calibration, the O 1s peak from O atoms in a bulk TiO_2 crystal (O_{bulk} atoms) was corrected to 530.3 eV. The spectra were deconvoluted into mixed Gaussian−Lorentzian curves (70:30) following Shirley-type background subtraction.

Results and discussion

A wide-scan XPS spectrum of the control, a (1×1) surface immersed in Milli-Q water for 1 day, is shown in Figure 2 (spectrum (a)). The intense peaks at ~460 and ~530 eV are Ti 2p and O 1s peaks, respectively. Ar and C peaks were also detected. The residue from sputtering explain the Ar atoms, and the C atoms result from the adventitious contaminants. Spectrum (b) was obtained using the (1×1) surface that was immersed in HBSS for 1 day. In addition to the Ti, O, Ar, and C peaks, Ca and P peaks were observed. Elements other than P and Ca included in the HBSS, such as Cl, Mg, S, K, and Na, were not detected, consistent with previous studies [3,4].

Figure 3 shows the narrow-scan spectra of the (1×1) surfaces that were immersed in either Milli-Q water or HBSS. The vertical scales of the spectra were normalized with respect to the height of the Ti 2p3/2 peak in each set of spectra. Spectra (a) were obtained from the surface that was immersed in Milli-Q water for 1 day. The O 1s spectrum shows an intense peak resulting from the O_{bulk} atoms. The shoulder on the high-binding-energy side of the O_{bulk} peak originates from low-coordination O atoms, OH groups, OOH groups, and contaminants [13]. The Ti 2p3/2 peak lacks the low-binding-energy shoulder originating from Ti cations with lower valence states, Ti^{n+} ($n<4$) [14], indicating that the (1×1) surface was stoichiometric. The surface O vacancies of low density should have been healed by the dissociative adsorption of H_2O molecules upon exposure to laboratory air. The C 1s spectrum is composed of three peaks at 285.5, 286.9, and 289.0 eV, which are assigned to C atoms involved in C–C/C–H, C–O, and O–C=O bonds ($C_{C\text{-}C/C\text{-}H}$, $C_{C\text{-}O}$, and $C_{O\text{-}C=O}$ atoms), respectively [15]. No feature could be observed in the P 2p and Ca 2p regions.

Spectra (b) were obtained from the surface immersed in the HBSS for 1 sec. The shoulder of the O_{bulk} peak slightly grew at ~531.6 and ~534.0 eV. The growth of the shoulder was highlighted by the O 1s spectrum in (a), which is represented by a gray line. The Ti 2p3/2 spectrum in (b) matches well the spectrum in (a), thus concealing the spectrum shown in (a), which is represented by a gray line. A single hump in the P 2p spectrum appeared at ~133.7 eV, and two humps appeared at 347.8 and 351.4 eV in the Ca 2p spectrum. A specific change in the C 1s spectrum relative to that shown in (a) was not observed.

Spectra (c) were obtained with the surface immersed in the HBSS for 5 sec. The components of the O 1s spectrum at 531.6 and 534.0 eV became intense. The Ti 2p3/2 spectrum remained similar to the previous spectra and thus fit with that obtained in (a). The hump in the P 2p spectrum at 133.7 eV became a distinct peak. The spectrum was fitted by two component peaks with an intensity ratio of 2:1 and a binding energy difference of 0.9 eV. The P atoms were in an identical chemical state

with a single pair of spin-orbit split peaks. The Ca 2p peaks at 347.8 and 351.4 eV became intense. The C 1s spectrum still did not show major changes.

P atoms on the (1×1) surface are in a phosphate species form. The binding energy of the P 2p peak at 133.7 eV was lower than that of the Ti 2p3/2 peak by 325.4 eV. This difference agrees with that previously determined for calcium phosphates on TiO_2, namely 325.2–325.4 eV [4]. According to Connor et al [16], a major form of adsorbed phosphate species in the aqueous solution with pH of 7.0–7.6 is the phosphate ion. The components of the O 1s shoulder at 531.6 and 534.0 eV are attributed to the phosphate ions. The binding energy differences from the O_{bulk} peaks at 1.3 and 3.7 eV agree with the growth of the O 1s shoulder induced by the phosphate ion, which ranges from 1.0 to 4.0 eV, as reported by Zhao et al [17]. The absence of Ti^{n+} ($n < 4$) shoulders in the Ti 2p3/2 peak indicates that phosphate ion adsorption does not reduce Ti_{5c} atoms. This independence of the Ti 2p3/2 peak shape from the adsorption of molecules has been reported upon for the adsorption of trimethyl acetic acid [18], methanol [19], and malonic acid [20]. The Ca atoms on the (1×1) surface are in a divalent state. The binding energy difference between the Ca 2p3/2 and Ti 2p3/2 peaks at 111.3 eV agrees with a difference of 111.2–111.3 eV for the calcium phosphates on TiO_2 [4].

Extending the immersion time to 1 min and 1 hr caused no notable change in the spectra, as shown in (d) and (e). Hence, the phosphate ions and the Ca ions were the major ad-species from the HBSS within the 1 hr immersion. Further extension of the immersion to 1 day and 1 week induced distinct changes in the O 1s, Ca 2p, and C 1s spectra, as shown in (f) and (g). A new peak appeared in the O 1s spectra at ~533.1 eV. The intensity of the Ca 2p peaks decreased with the immersion time in comparison with those in (e). The intensity of the $C_{C\text{-}O}$ peak increased relative to that of the $C_{C\text{-}C/C\text{-}H}$ peak.

The distinct growth of the $C_{C\text{-}O}$ peak after the 1-day and 1-week immersions is attributed to an increase in glucose. The binding energy difference between the $C_{C\text{-}O}$ and the $C_{C\text{-}C/C\text{-}H}$ peaks of 1.4 eV agrees with that previously reported for glucose, 1.5 eV [21]. The peak at 533.1 eV in the O 1s spectra that appeared along with the growth of the $C_{C\text{-}O}$ peak is assigned to the OH groups of the glucose.

By assuming that the P and Ca atoms were uniformly distributed on the surface, their coverages are estimated by referring to the work of Peng et al [22]. For P atoms,

$$\frac{I_P}{I_{Ti}} = \frac{\sigma_P N_P}{\sigma_{Ti} N_{Ti} \sum_{n=1}^{\infty} exp\left[\frac{-(n-1)d}{\lambda cos\theta}\right]} \approx \frac{\sigma_P N_P}{\sigma_{Ti} N_{Ti}\left[1-exp\left(\frac{-d}{\lambda cos\theta}\right)\right]^{-1}} \quad (1)$$

where I_p/I_{Ti} is the intensity ratio of the P 2p3/2 peak with respect to the Ti 2p3/2 peak. σ and N are the photoionization cross section and the density of the atoms, respectively. σ values of 0.789, 3.35, and 5.22 were used for P 2p3/2, Ca 2p3/2, and Ti 2p3/2 photoelectrons [23], respectively. N_{Ti} is the density of Ti atoms in the TiO_2 layers along the [110] axis, 10.26 nm^{-2}. d is the distance between the adjacent TiO_2 layers, 0.33 nm. λ is the inelastic mean free path of the Ti 2p photoelectrons in bulk TiO_2, 1.54 nm [24]. The screening effect of the P and Ca atoms for the Ti 2p photoelectrons is ignored. Figure 4 shows N_p and N_{Ca} calculated by equation (1) for the surfaces with different immersion times. N_p increased with the immersion time up to 1 min to a value of ~3.8 nm^{-2} and remained relatively constant for 1 week (6% fluctuation). On the other hand, N_{Ca} reached a value of 3.2 nm^{-2} after 60 sec of immersion and decreased with further immersion. Compared with the surface immersed for 60 sec, the average N_{Ca} decreased by ~15% after a 1 hr immersion and by ~74% after a 1 week immersion.

The co-adsorption of the phosphate ions and Ca ions suggests that the charges induced by their adsorption were balanced in the HBSS. The pH of the point of zero charge of the (1×1) surface is expected to be ~4.8 on the basis of a sum-frequency-generation study of the air-annealed (110) surface by Fitts et al [25]. Therefore, the (1×1) surface covered by a water layer in laboratory air is negatively charged and is rich in the OH_t group. In the HBSS that has a pH of 7.0–7.6, the phosphate ions replace the OH_t groups and bond to the Ti_{5c} atoms [26]. One phosphate ion enhances two negative charges when replacing one OH_t group.

$$Ti - OH_t^- + PO_4^{3-} \rightarrow Ti - PO_4^{3-} + OH^- \qquad (R1)$$

One negative charge increases when one phosphate ion replaces two OH_t groups.

$$2(Ti - OH_t^-) + PO_4^{3-} \rightarrow Ti - (PO_4^{3-}) - Ti + 2OH^- \qquad (R2)$$

The possible adsorption configurations of the phosphate ions are bidentate chelating and bidentate bridging [16]. Hence, the adsorbed phosphate ions in reactions 1 and 2 are in the bidentate chelating and bidentate bridging coordinations, respectively. When the N_{Ca}/N_p ratio is roughly estimated to be 3/4 on the surfaces after immersion for 1 hr or less, the positive charges from Ca ions are compensated for by phosphate ions with an equal proportion of the bidentate chelating and bidentate

bridging forms. On the other hand, the N_{Ca} distinctly decreased in immersions lasting 1 hr and longer. The decrease in the N_{Ca} may be explained by assuming that the bidentate bridging form becomes dominant with the extension of the immersion time.

The distribution and arrangement of the ad-species were examined by STM. Figure 5a shows the control (1×1) surface immersed in Milli-Q water for 1 day. The surface showed the same step-terrace structure before the removal from UHV (Figure 1b), but the terraces were covered by molecule-sized spots. The spots are classified into three kinds of O-containing species according to their heights. The highest spots are the hydroperoxyl (OOH) group with an "up-conformation" in which the OOH plane is parallel to the [001] direction, the middle spots are the OH_t group, and the lowest spots are the OOH group with a "transverse conformation" in which the OOH plane is normal to the [001] direction [10,13]. The OH_t groups and the OH_b groups are formed by dissociation of H_2O molecules when the wet (1×1) surface is introduced to UHV [13]. A part of the OH_b groups react with O_2 to form the OOH groups. The OH_t groups and the OOH groups are bonded to the Ti_{5c} atoms, and some of them are arranged in a (2×1) periodicity indicated by the 0.60 nm × 0.65 nm rectangle in the inset of the figure. The density of the O-containing species was 1.8 nm^{-2}. Non-uniform bright species, such as the two indicated by the arrows, are adventitious contaminants.

Figure 5b shows the (1×1) surface immersed in HBSS for 1 sec. Ragged spots with diameters smaller than those of the O-containing species appeared. A part of the ragged spots resembled strings extended in the $[1\bar{1}0]$ direction, as indicated by the rectangle in the inset of the figure. The ragged spots were shorter than the OH_t groups by 0.05 nm and had a height equivalent to that of the transverse OOH groups. Spots with a clear-cut outline on the left half of the inset are the O-containing species. Along with the emergence of the ragged spots, the density of the O-containing species decreased to 0.52 nm^{-2}. It was difficult to count the ragged spots because of their fuzzy outlines. Figure 5c shows the (1×1) surface immersed in HBSS for 5 sec. The area covered with the ragged spots increased, and the density of the O-containing species decreased to 0.46 nm^{-2}. When the immersion time was extended to 1 min, the area covered with the ragged spots further increased, and the density of the O-containing species decreased to 0.29 nm^{-2}, as shown in Figure 5d. The inset shows the area where the Ti_{5c} atom rows were accidentally exposed, which indicates the monolayer thickness of the phosphate ions. A part of the ragged spots was arranged in a (2×1) periodicity as indicated by the rectangle. While 1 hr immersion did not cause a distinct change in surface topography (Figure 5e), bright species with a non-uniform shape increased after the

immersions for 1 day and 1 week, as shown in Figure 5f and 5g. The ragged spots were observed through the breaks of the bright species.

The ragged spots are assigned to the presence of phosphate ions. The areas covered by the ragged spots were equivalent on the surfaces immersed in HBSS for 1 min and longer, in agreement with the relatively constant N_p on these surfaces. N_p is saturated when the phosphate ions occupy the Ti_{5c} atoms to form a monolayer. The images of the phosphate ions occasionally changed, depending on the tip condition. Figure 5h shows the change in the image of the phosphate ions. The phosphate ions can be observed as spots in the upper half of the image. Some of the spots were elongated in the [1$\bar{1}$0] direction, but the string-like appearance is limited. The tip condition changed in the scan line indicated by the arrows, and the phosphate ions had a string-like appearance in the lower half of the image. The elongated shape of the phosphate ions probably reflects the spatial distribution of the lowest unoccupied molecular orbital (LUMO) closest to the tip. Our preliminary calculation for using the B3LYP method and the 6-311++G** basis sets showed that the LUMO of the phosphate ion isolated in space is localized around the O atoms. When a phosphate ion bonds to two Ti_{5c} atoms in the bidentate configuration, two free O atoms extend laterally in the [1$\bar{1}$0] direction. Hence, the LUMO around the two O atoms likely produce the spots aligned in the [1$\bar{1}$0] direction, although a more precise modeling including the TiO_2 substrate is necessary in order to understand the STM image.

The strings extended in the [1$\bar{1}$0] direction originate from the phosphate ions arranged in phase with the neighbors on the adjacent Ti_{5c} atom rows. Hence, a major part of the phosphate ions are expected to be arranged in the (2×1) periodicity with respect to the (1×1) surface. Actually, the half-order spots along the <001> directions emerged in the LEED patterns, as indicated by the arrows in Figure 6. The (2×1) arrangement is known to exist in the case of carboxylate molecules ($R–COO^-$) [27–31].

The density of the phosphate ions is 2.6 nm^{-2} when they occupy the Ti_{5c} atoms to form a (2×1) monolayer. On the other hand, the maximum N_p from the XPS analysis was 3.8 nm^{-2} and exceeded the density of 2.6 nm^{-2}. This deviation stemmed from the model used to develop equation 1, in which the attenuation of Ti 2p3/2 photoelectrons in the phosphate ion layer is ignored. Because λ is smaller than it actually is, the denominator of the right-hand side of equation 1 provides a value larger than that should be in actuality, which results in an overestimation of N_p and N_{Ca}.

Ca ions are unlikely to exist as ragged spots. The N_{Ca} decreased to less than half between immersions of 1 min and 1 week. This decrease disagrees with the density of the ragged spots, even

if we consider only the area free of the bright species in the case of the surface immersed for 1 week. According to the density functional theory calculations by San Miguel et al., the 3-fold hollow consisting of two O_b atoms and one in-plane O atom is the most energetically favorable site for Ca atoms [32]. Molecular dynamics simulation by Předota et al. [33] showed that Ca ions in aqueous solution are stabilized at hollow sites composed of O_b atoms and O atoms of the OH_t groups. Ca ions from the HBSS are probably adsorbed at the hollow sites of O atoms. The O atoms of adsorbed phosphate ions instead of the OH_t groups may constitute the hollow sites. The Ca ions are separated from the tip more than the topmost O atoms of the phosphate ions; therefore, electron tunneling to the Ca ions would contribute less to the formation of the image contrast.

Bicarbonate ions (HCO_3^-) also form a monolayer with (2×1) periodicity [34], but are inappropriate for assignment as the ragged spots from the HBSS. The infrared adsorption spectrum of the TiO_2 film shows replacement of adsorbed carbonate species with phosphate ions after immersion in the Na_2HPO_4 solution [16]. The phosphate ions are more strongly coordinated to the TiO_2 surface than are the bicarbonate ions.

The non-formation of calcium phosphate on the (1×1) surface contrasts with the formation of calcium phosphate on the (110) surface annealed in air [35]. There could be structures specific to the air-annealed surface that act as growth sites of calcium phosphate, although they are unclear at present. The non-formation of calcium phosphate on the (1×1) surface is hypothetically explained by epitaxial growth of the brushite. Brushite, a candidate precursor phase of hydroxyapatite [2,5], consists of $CaHPO_4$ sheets and H_2O bilayers that are alternately stacked along the [010] direction, as shown in Figure 7a. Assuming that the hydrogen phosphate ions are arranged on the (1×1) surface, the least mismatch is attained on the (010) surface of the brushite. Figure 7b shows the (010) surface of the $CaHPO_4$ sheet indicated by the asterisk in Figure 7a. The hydrogen phosphate ions on the (1×1) surface need to be arranged in the c(2×2) structure, where the ions are out of phase with the neighboring ions in the adjacent Ti_{5c} atom rows, and the [001] direction on the (1×1) surface is the [100] direction of the $CaHPO_4$ sheet. The c(2×2) arrangement of the hydrogen phosphate ions is enabled by the migration along the Ti_{5c} atom rows. The hydrogen phosphate ions in the c(2×2) arrangement form a parallelogram with a short side of 0.60 nm, a long side of 0.72 nm, and a larger interior angle of 114.8°. The parallelogram is displayed in Figure 7b. The short side and the larger interior angle of the parallelogram match the lattice constant a and the interaxial angle β of brushite, with deviations of ~3%. However, the mismatch between the long side of the parallelogram and the

lattice constant *c* of the brushite reaches as high as 15%. This large deviation is unfavorable for the coordination of Ca ions to the hydrogen phosphate ions.

Conclusion

Phosphate ions from the HBSS produced a monolayer on the (1×1) surface. Calcium phosphate did not form with 1-week immersion, inconsistent with the osteoconductivity of TiO_2. Arrangement of the phosphate ions suitable for the epitaxial growth of the brushite could not be attained on the (1×1) surface.

The above results prove that the growth of calcium phosphate on TiO_2 is sensitive to lattice matching between the two surfaces. The effects of point defects such as O vacancies, OH groups, and Ti interstitials are possible nanostructures that affect the osteoconductivity and are subjects to be examined. Thus, the use of a well-defined single crystal surface was demonstrated to be beneficial in gaining a microscopic view of the osteoconductivity of TiO_2.

Acknowledgment

This work was supported by the Grants-in-Aid for Scientific Research from the Japanese Society for the Promotion of Science KAKENHI (grant numbers 26600024, 26630330, 24246014, and 16K13624).

References

[1] D.M. Brunette, P. Tengvall, M. Textor, P. Thomsen (Eds.), Titanium in Medicine, Springer, Berlin, 2001.

[2] S.V. Dorozhkin, M. Epple, Biological and medical significance of calcium phosphates, Angew. Chem. Int. Ed. 41 (2002) 3130–3146.

[3] T. Hanawa, M. Ota, Characterization of surface film formed on titanium in electrolyte using XPS, Appl. Surf. Sci. 55 (1992) 269–276.

[4] T. Hanawa, M. Ota, Calcium phosphate naturally formed on titanium in electrolyte solution, Biomaterials, 12 (1991) 767–774.

[5] C.C. Chusuei, D.W. Goodman, M.J. Van Stipdonk, D.R. Justes, K.H. Loh, E.A. Schweikert, Solid-liquid adsorption of calcium phosphate on TiO_2, Langmuir 15 (1999) 7355–7360.

[6] T. Kokubo, D.K. Pattanayak, S. Yamaguchi, H. Takadama, T. Matsushita, T. Kawai, M. Takemoto, S. Fujibayashi, T. Nakamura, Positively charged bioactive Ti metal prepared by simple chemical and heat treatments, J. R. Soc. Interface 7 (2010) S503–S513.

[7] C.L. Pang, R. Lindsay, G. Thornton, Chemical reactions on rutile TiO_2(110), Chem. Soc. Rev. 37 (2008) 2328−2353.

[8] H. Onishi, K. Fukui, Y. Iwasawa, Atomic-scale surface structures of TiO_2(110) determined by scanning tunneling microscopy: A new surface-limited phase of titanium oxide, Bull. Chem. Soc. Jpn. 68 (1995) 2447−2458.

[9] S. Wendt, R. Schaub, J. Matthiesen, E.K. Vestergaard, E. Wahlström, M.D. Rasmussen, P. Thostrup, L.M. Molina, E. Lægsgaard, I. Stensgaard, B. Hammer, F. Besenbacher, Oxygen vacancies on TiO_2(110) and their interaction with H_2O and O_2: a combined high-resolution STM and DFT study, Surf. Sci. 598 (2005) 226–245.

[10] Y. Du, N.A. Deskins, Z. Zhang, Z. Dohnálek, M. Dupuis, I. Lyubinetsky, Imaging consecutive steps of O_2 reaction with hydroxylated TiO_2(110): identification of HO_2 and terminal OH intermediates, J. Phys. Chem. C 113 (2009) 666–671.

[11] H. Tatsumi, A. Sasahara, M. Tomitori, Lateral distribution of Li atoms at the initial stage of adsorption on TiO_2(110) surface, J. Phys. Chem. C 116 (2012) 13688–13692.

[12] A. Sasahara, S. Kitamura, H. Uetsuka, H. Onishi, Oxygen-atom vacancies imaged by a noncontact atomic force microscope operated in an atmospheric pressure of N_2 gas, J. Phys. Chem. B 108 (2004) 15735–15737.

[13] A. Sasahara, M. Tomitori, An atomic-scale study of TiO_2(110) surfaces exposed to humid

environments, J. Phys. Chem. C 120 (2016) 21427−21435.

[14] A. Sasahara, M. Tomitori, XPS and STM study of Nb-doped TiO_2(110)-(1×1) surfaces, J. Phys. Chem. C 117 (2013) 17680−17686.

[15] E. McCafferty, J.P. Wightman, Determination of the concentration of surface hydroxyl groups on metal oxide films by a quantitative XPS method, Surf. Interface Anal. 26 (1998) 549–564.

[16] P.A. Connor, A.J. McQuillan, Phosphate adsorption onto TiO_2 from aqueous solutions: an in situ internal reflection infrared spectroscopic study, Langmuir 15 (1999) 2916–2921.

[17] D. Zhao, C. Chen, Y. Wang, H. Ji, W. Ma, L. Zang, J. Zhao, Surface modification of TiO_2 by phosphate: effect on photocatalytic activity and mechanism implication, J. Phys. Chem. C 112 (2008) 5993–6001.

[18] J.M. White, J. Szanyi, M.A. Henderson, Thermal chemistry of trimethyl acetic acid on TiO_2(110), J. Phys. Chem. B 108 (2004) 3592–3602.

[19] P.M. Jayaweera, E.L. Quah, H. Idriss, Photoreaction of ethanol on TiO_2(110) single-crystal surface, J. Phys. Chem. C 111 (2007) 1764–1769.

[20] K.L. Syres, A.G. Thomas, D.M. Graham, B.F. Spencer, W.R. Flavell, M.J. Jackman, V.R. Dhanak, Adsorption and stability of malonic acid on rutile TiO_2 (110), studied by near edge X-ray absorption fine structure and photoelectron spectroscopy, Surf. Sci. 626 (2014) 14–20.

[21] S. Dahle, J. Meuthen, W. Viöl, W. Maus-Friedrichs, Adsorption of silver on glucose studied with MIES, UPS, XPS and AFM, Appl. Surf. Sci. 284 (2013) 514–522.

[22] X.D. Peng, M.A. Barteau, Characterization of oxide layers on Mg(0001) and comparison of H_2O adsorption on surface and bulk oxides, Surf. Sci. 233 (1990) 283–292.

[23] J.H. Scofield, Hartree-slater subshell photoionization cross-sections at 1254 and 1487 eV, J. Electron Spectrosc. Relat. Phenomena 8 (1976) 129–137.

[24] G.G. Fuentes, E. Elizalde, F. Yubero, J.M. Sanz, Electron inelastic mean free path for Ti, TiC, TiN and TiO_2 as determined by quantitative reflection electron energy-loss spectroscopy, Surf. Interface Anal. 33 (2002) 230–237.

[25] J.P. Fitts, M.L. Machesky, D.J. Wesolowski, X. Shang, J.D. Kubicki, G.W. Flynn, T.F. Heinz, K.B. Eisenthal, Second-harmonic generation and theoretical studies of protonation at the water/α-TiO_2 (110) interface, Chem. Phys. Lett. 411 (2005) 399–403.

[26] K.E. Healy, P.D. Ducheyne, Hydration and preferential molecular adsorption on titanium in vitro, Biomaterials 13 (1992) 553–561.

[27] Z.-T. Wang, J.C. Garcia, N.A. Deskins, I. Lyubinetsky, Ability of TiO_2(110) surface to be fully hydroxylated and fully reduced, Phys. Rev. B 92 (2015) 081402(R) 1−5.

[28] J.S. Prauzner-Bechcicki, S. Godlewski, A. Tekiel, P. Cyganik, J. Budzioch, M. Szymonski, High-resolution STM studies of terephthalic acid molecules on rutile TiO_2(110)-(1×1) surfaces, J. Phys. Chem. C 113 (2009) 9309–9315.

[29] T. Qiu, M.A. Barteau, STM study of glycine on TiO_2(110) single crystal surfaces, J. Coll. Int. Sci. 303 (2006) 229–235.

[30] A. Sasahara, H. Uetsuka, T. Ishibashi, H. Onishi, The dependence of scanning tunneling microscope topography of carboxylates on their terminal groups, J. Phys. Chem. B 107 (2003) 13925–13928.

[31] Q. Guo, E.M. Williams, The effect of adsorbate-adsorbate interaction on the structure of chemisorbed overlayers on TiO_2(110), Surf. Sci. 433–435 (1999) 322–326.

[32] M.A. San Miguel, J. Oviedo, J.F. Sanz, Ca deposition on TiO_2(110) surfaces: insights from quantum calculations, J. Phys. Chem. C 113 (2009) 3740–3745.

[33] M. Předota, Z. Zhang, P. Fenter, D.J. Wesolowski, P.T. Cummings, Electric double layer at the rutile (110) surface. 2. adsorption of ions from molecular dynamics and X-ray experiments, J. Phys. Chem. B 108 (2004) 12061−12072.

[34] A. Song, E.S. Skibinski, W.J.I. DeBenedetti, A.G. Ortoll-Bloch, M.A. Hines, Nanoscale solvation leads to spontaneous formation of a bicarbonate monolayer on rutile (110) under ambient conditions: implications for CO_2 photoreduction, J. Phys. Chem. C 120 (2016) 9326−9333.

[35] M. Murphy, M.S. Walczak, H. Hussain, M.J. Acres, C.A. Muryn, A.G. Thomas, N. Silikas, R. Lindsay, An ex situ study of the adsorption of calcium phosphate from solution onto TiO_2(110) and Al_2O_3(0001), Surf. Sci. 646 (2016) 146–153.

Figure captions

Figure 1. (a) A ball-and-stick model of the TiO_2(110)-(1×1) surface. Light-blue balls and red balls represent Ti atoms and O atoms, respectively. The smallest gray balls bound to the O atoms represent H atoms. The OH_t group terminating the Ti_{5c} atom is added for reference. The unit cell indicated by the dotted line has dimensions of 0.30 nm × 0.65 nm. (b,c) STM images of the (1×1) surface. Scan sizes are (b) 40 nm × 40 nm and (c) 5 nm × 5 nm. Sample bias voltage, +1.4 V; tunneling current, 0.2 nA.

Figure 2. Wide-scan XPS spectra of the (1×1) surfaces immersed in (a) Milli-Q water and (b) HBSS. The immersion period was 1 day for both surfaces.

Figure 3. Sets of O 1s, Ti 2p3/2, Ca 2p, C 1s, and P 2p XPS spectra of the (1×1) surfaces. (a) The surface immersed in Milli-Q water for 1 day. (b–g) The surfaces immersed in HBSS for (b) 1 sec, (c) 5 sec, (d) 1 min, (e) 1 hr, (f) 1 day, and (g) 1 week. The O 1s and Ti 2p3/2 spectra in (b–g) are superimposed onto those in (a) represented by a gray line. The thin black lines in the P 2p spectrum in (c) represent two fitted component peaks and an envelope curve formed by them.

Figure 4. Dependence of the densities of P (open circles) and Ca (solid circles) atoms on the (1×1) surfaces on the immersion time in HBSS.

Figure 5. (a–g) STM images of the (1×1) surfaces with a size of 40 nm × 40 nm with close-ups of 5 nm × 5 nm. (a) The surface immersed in Milli-Q water for 1 day. (b–g) The surfaces immersed in HBSS for (b) 1 sec, (c) 5 sec, (d) 1 min, (e) 1 hr, (f) 1 day, and (g) 1 week. The squares in the insets in (a) and (d) indicate (2×1) unit cells. The number (i) signifies the OOH group with “up-conformation” (ii) is the OH_t group, and (iii) is OOH groups with “transverse conformation”. (h) The surface immersed in HBSS for 1 min (5 nm × 5 nm). The scan direction is right to left and top to bottom. The arrows indicate the scan line where the appearance of the spots accidentally changed. Sample bias voltage, +1.6 V; tunneling current, 0.2 nA.

Figure 6. LEED patterns of the (1×1) surfaces (a) before and (b) after immersion in HBSS for 1 min. Incident electron energies for (a) and (b) are 64 eV. Dotted rectangles represent the reciprocal unit cell of the (1×1) surface. Arrows in (b) indicate additional spots showing the (2×1) structure.

Figure 7. (a) A ball-and-stick model of a brushite crystal viewed from the [001] direction. Yellow, green, red, and gray balls respectively represent Ca, P, O, and H atoms. (b) Upper part of the $CaHPO_4$ sheet marked with an asterisk in (a). Upper and lower panels show views from the [010] and the [001] directions, respectively. The light blue parallelogram indicates the c(2×2) unit cell that is formed by four phosphate ions on the (1×1) surface.

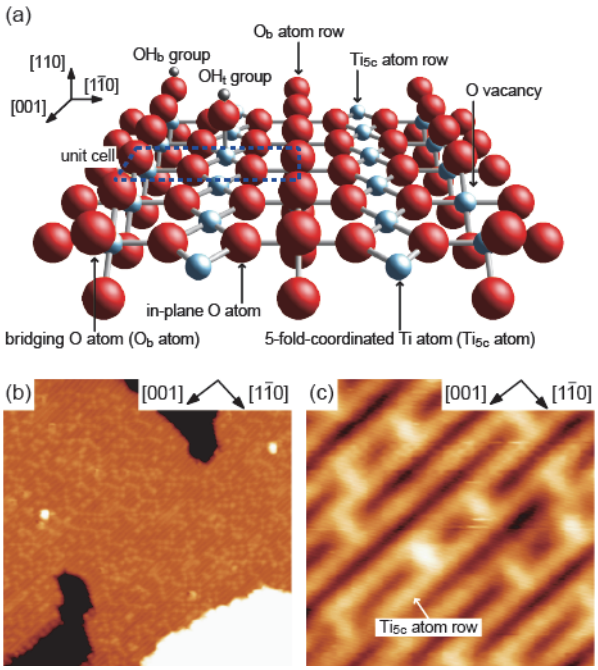

Figure 1. (a) A ball-and-stick model of the TiO_2(110)-(1×1) surface. Light-blue balls and red balls represent Ti atoms and O atoms, respectively. The smallest gray balls bound to the O atoms represent H atoms. The OH_t group terminating the Ti_{5c} atom is added for reference. The unit cell indicated by the dotted line has dimensions of 0.30 nm × 0.65 nm. (b,c) STM images of the (1×1) surface. Scan sizes are (b) 40 nm × 40 nm and (c) 5 nm × 5 nm. Sample bias voltage, +1.4 V; tunneling current, 0.2 nA.

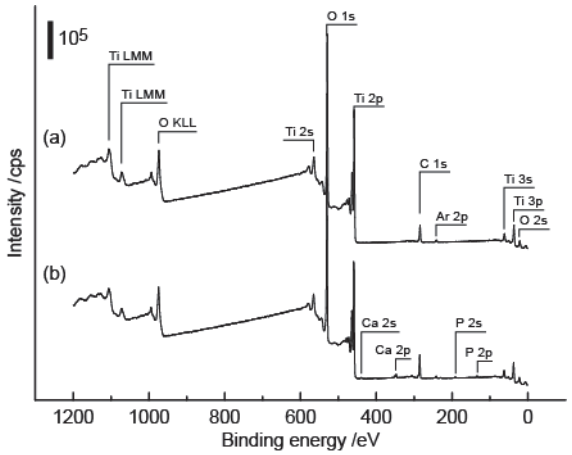

Figure 2. Wide-scan XPS spectra of the (1×1) surfaces immersed in (a) Milli-Q water and (b) HBSS. The immersion period was 1 day for both surfaces.

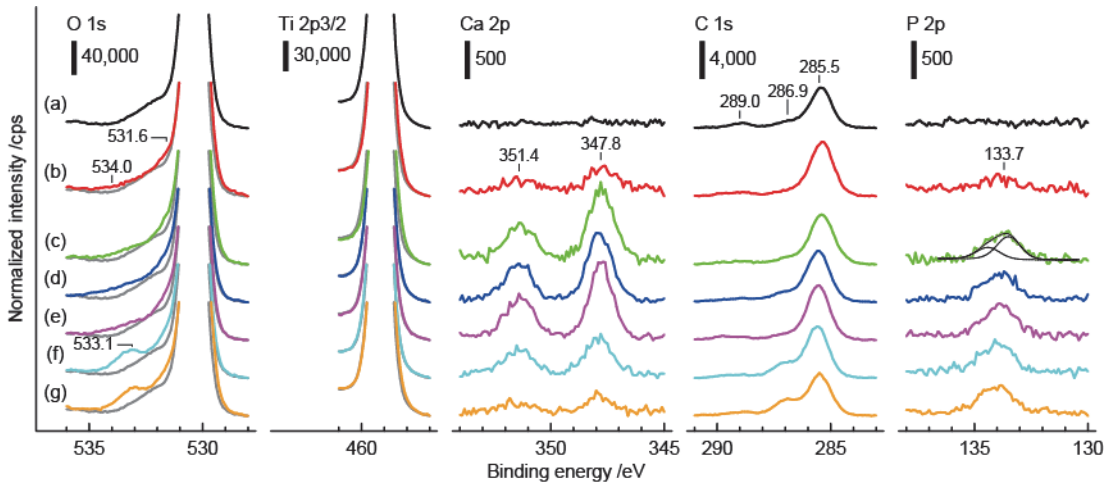

Figure 3. Sets of O 1s, Ti 2p3/2, Ca 2p, C 1s, and P 2p XPS spectra of the (1×1) surfaces. (a) The surface immersed in Milli-Q water for 1 day. (b–g) The surfaces immersed in HBSS for (b) 1 sec, (c) 5 sec, (d) 1 min, (e) 1 hr, (f) 1 day, and (g) 1 week. The O 1s and Ti 2p3/2 spectra in (b–g) are superimposed onto those in (a) represented by a gray line. The thin black lines in the P 2p spectrum in (c) represent two fitted component peaks and an envelope curve formed by them.

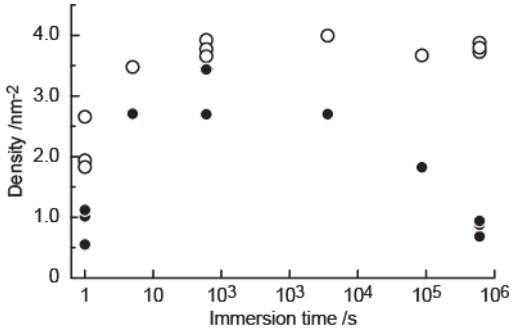

Figure 4. Dependence of the densities of P (open circles) and Ca (solid circles) atoms on the (1×1) surfaces on the immersion time in HBSS.

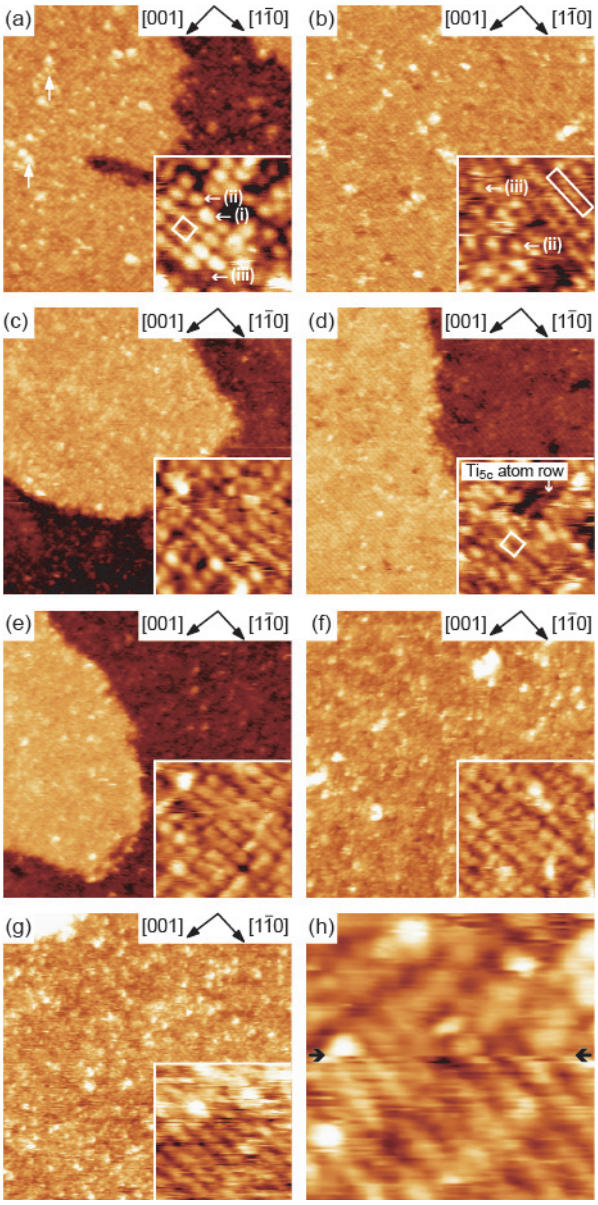

Figure 5. (a–g) STM images of the (1×1) surfaces with a size of 40 nm × 40 nm with close-ups of 5 nm × 5 nm. (a) The surface immersed in Milli-Q water for 1 day. (b–g) The surfaces immersed in HBSS for (b) 1 sec, (c) 5 sec, (d) 1 min, (e) 1 hr, (f) 1 day, and (g) 1 week. The squares in the insets in (a) and (d) indicate (2×1) unit cells. The number (i) signifies the OOH group with "up-conformation" (ii) is the OH_t group, and (iii) is OOH groups with "transverse conformation". (h) The surface immersed in HBSS for 1 min (5 nm × 5 nm). The scan direction is right to left and top to bottom. The arrows indicate the scan line where the appearance of the spots accidentally changed. Sample bias voltage, +1.6 V; tunneling current, 0.2 nA.

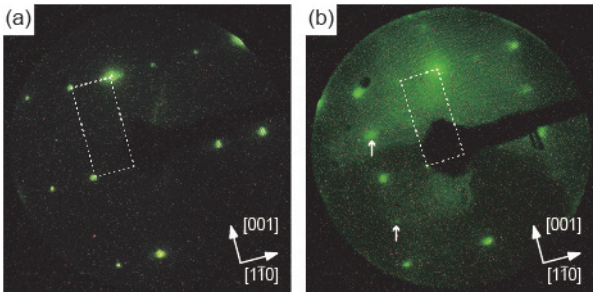

Figure 6. LEED patterns of the (1×1) surfaces (a) before and (b) after immersion in HBSS for 1 min. Incident electron energies for (a) and (b) are 64 eV. Dotted rectangles represent the reciprocal unit cell of the (1×1) surface. Arrows in (b) indicate additional spots showing the (2×1) structure.

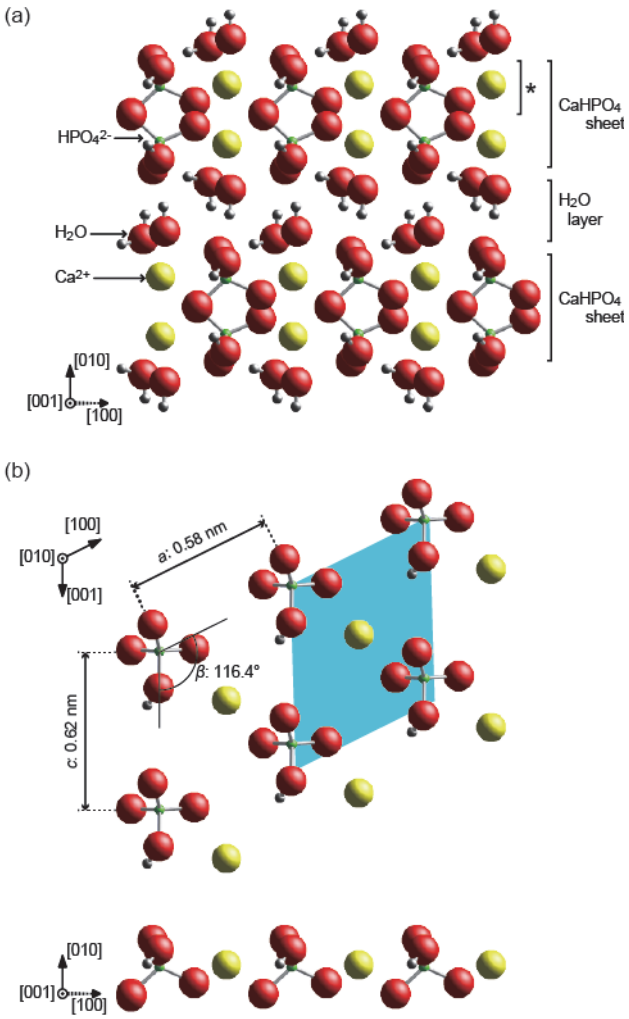

Figure 7. (a) A ball-and-stick model of a brushite crystal viewed from the [001] direction. Yellow, green, red, and gray balls respectively represent Ca, P, O, and H atoms. (b) Upper part of the $CaHPO_4$ sheet marked with an asterisk in (a). Upper and lower panels show views from the [010] and the [001] directions, respectively. The light blue parallelogram indicates the c(2×2) unit cell that is formed by four phosphate ions on the (1×1) surface.